Science
AAAS

Atmospheric Pco_2 Perturbations Associated with the Central Atlantic Magmatic Province

Morgan F. Schaller, *et al.*

Science **331**, 1404 (2011);
DOI: 10.1126/science.1199011

Atmospheric P_{CO_2} Perturbations Associated with the Central Atlantic Magmatic Province

Morgan F. Schaller,[1]* James D. Wright,[1] Dennis V. Kent[1,2]

The effects of a large igneous province on the concentration of atmospheric carbon dioxide (P_{CO_2}) are mostly unknown. In this study, we estimate P_{CO_2} from stable isotopic values of pedogenic carbonates interbedded with volcanics of the Central Atlantic Magmatic Province (CAMP) in the Newark Basin, eastern North America. We find pre-CAMP P_{CO_2} values of ~2000 parts per million (ppm), increasing to ~4400 ppm immediately after the first volcanic unit, followed by a steady decrease toward pre-eruptive levels over the subsequent 300 thousand years, a pattern that is repeated after the second and third flow units. We interpret each P_{CO_2} increase as a direct response to magmatic activity (primary outgassing or contact metamorphism). The systematic decreases in P_{CO_2} after each magmatic episode probably reflect consumption of atmospheric CO_2 by weathering of silicates, stimulated by fresh CAMP volcanics.

Large igneous provinces (LIPs) are geologically rapid episodes of extensive volcanism, often flooding vast oceanic or continental regions with several million cubic kilometers of lava (*1*). In particular, continental flood basalts have the potential to directly perturb Earth's climate system through the emission of gasses to the atmosphere: most notably, SO_2 and CO_2, which together may result in an immediate (1- to 10-year) cooling (*2*, *3*), followed by a longer-term (10^2- to 10^5-year) warming (*4*). Of these, only CO_2 has the potential to influence climate on both short and long time scales because of its relatively long atmospheric residence time and effectiveness as a greenhouse gas, leading some to conclude that CO_2 is the primary driver of Phanerozoic climate (*5*).

If the concentration of atmospheric CO_2 exerts an influence on climate over such broad time scales, what are the effects of a LIP on this essential parameter of the carbon cycle? Although the potential radiative effects of LIP CO_2 degassing on the million-year scale have been considered inconsequential (*6*, *7*), shorter (10^4- to 10^5-year)–time scale reconstructions of atmospheric partial pressure of CO_2 (P_{CO_2}) before and after LIP eruptions have not been systematically determined because of inadequate chronostratigraphic resolution in most settings (*8*, *9*). Consequently, the direct P_{CO_2} effect of a LIP remains untested empirically.

Intriguingly, LIP volcanism is often temporally associated with mass extinction events throughout Earth's history (*10*). The three largest continental LIPs of the Phanerozoic are the Siberian Traps, the Central Atlantic Magmatic Province (CAMP), and the Deccan Traps, each of which is linked to one of the "Big 5" Phanerozoic mass extinctions [the end-Permian, end-Triassic, and the Cretaceous–Paleogene events, respectively] (*11*, *12*). Though attempts have been made to estimate the gaseous emissions attributable to the Deccan (*6*, *13*, *14*) and Siberian (*15*, *16*) traps, it is difficult to demonstrate causality because the uncertainties in correlating these P_{CO_2} estimates from afar to the volcanic stratigraphy itself are usually no better than the turnover time of an atmospheric P_{CO_2} perturbation (*17*). Of these, only the CAMP is sequenced in high-resolution, temporally continuous sediments that contain paleosols appropriate for estimating P_{CO_2} and have a well-established chronology (*18*, *19*) and extinction level.

Extrusives from the CAMP (*20*) are preserved in direct stratigraphic succession with cyclic continental sediments in the Newark Basin of eastern North America (Fig. 1). Milankovitch cyclostratigraphy of the primarily lacustrine sediments interbedded within the CAMP extrusives have yielded precise age control (to the level of orbital precession) and an estimated total volcanic duration of ~600 ± 20 thousand years (ky) (*21*, *22*). In this same Newark Basin section, palynofloral evidence of the end-Triassic extinction (ETE) is found stratigraphically just below the first of the CAMP volcanics, preceding the magmatism by ~20 ky [(*23*), see (*24*) for review]. Also interspersed throughout these sediments, and often forming from CAMP lava flows themselves, are pedogenic carbonate-bearing paleosols (Fig. 2, A and B), which can be used to estimate ancient atmospheric P_{CO_2} (*25*). Thus, the Newark stratigraphy is ideally situated to directly test the P_{CO_2} effect of a LIP. Previous attempts at reconstructing the P_{CO_2} effect associated with CAMP extrusives had very sparse sampling resolution (*26*) or had to rely on imprecise long-distance correlation (*8*, *9*).

We use $\delta^{13}C$ measurements of pedogenic carbonate nodules from paleosols stratigraphically distributed before and after each extrusive unit to generate a high-resolution P_{CO_2} record through the Newark Basin CAMP sequence (Fig. 1). The extrusion of ~2 to 4 × 10^6 km^3 of volcanics (*27*, *28*) in less than 1 million years (My) implies a measurable effect on atmospheric P_{CO_2}, which our temporal resolution should allow us to detect. According to the model of Dessert *et al.* (*17*) scaled to the Deccan Traps, the transient increase in P_{CO_2} is on the time scale of the eruptions, after which continental silicate weathering should lower P_{CO_2} to pre-eruption levels in ~1 My.

Estimating P_{CO_2} from pedogenic carbonates. Organic and inorganic carbon isotope measurements on paleosols from outcrop—and from multiple, stratigraphically overlapping cores taken by the Army Corps of Engineers (ACE) through the extrusive interval (fig. S1) (*29*)—are used as inputs into the diffusion model of Cerling (*30*)

$$C_a = S(z)\frac{\delta_s - 1.0044\delta_\phi - 4.4}{\delta_a - \delta_s} \quad (1)$$

[1]Department of Earth and Planetary Sciences, Rutgers University, Piscataway, NJ 08854, USA. [2]Lamont-Doherty Earth Observatory of Columbia University, Palisades, NY 10964, USA.

*To whom correspondence should be addressed. E-mail: schaller@rci.rutgers.edu

Fig. 1. (**A**) Stratigraphy and lithology (*22*, *34*, *41*) of the upper Newark Basin stratigraphic section, based on assembly of a series of short cores taken by the ACE covering the extrusive interval in high resolution (*49*), with substantial overlap both internally and with the Newark Basin Coring Project (NBCP) Martinsville core (*19*, *22*) and outcrop. Note that the ETE event (red) is several meters below the equivalent of the Orange Mountain Basalt (OMB, the first flow unit) in the Jacksonwald section of the Newark Basin (*24*). Stratigraphic thickness is scaled arbitrarily from the base of the laterally extensive OMB. J, Jurassic; Tr, Triassic; UU through MM are stratigraphic members. (**B**) Profile-equilibrated mean $\delta^{13}C$ values of pedogenic carbonate in the Newark stratigraphic section. Error is ±SD of mean (Fig. 2 and table S1) (*29*). Circles, samples from core; squares, outcrop. PDB, Pee Dee belemnite. (**C**) Measured $\delta^{13}C$ values of preserved soil organic matter from clay linings or as close to the paleosol surface as possible. (**D**) Results of the pedogenic carbonate paleobarometer based on the input variables from (B) and (C) at 25°C. The concentration of respired CO_2 in the soil [$S(z)$] was estimated to be 3000 ± 1000 ppm (error bars), corresponding to a plausible range for midproductivity tropical soils and probably encompassing the range of calculated atmospheric P_{CO_2} values. Carbon-cycle perturbations are built into the model because the carbon isotopic ratio of the atmosphere (δ_a) is calculated from the measured $\delta^{13}C_{org}$ by: $\delta_a = (\delta^{13}C_{org} + 18.67)/1.10$ (*32*), which assumes consistent fractionation by photosynthesis [see (*29*) and table S1 for numerical values].

where C_a is the concentration of atmospheric CO_2, $S(z)$ is the concentration of CO_2 due to respiration of soil organic matter, δ_s is the $\delta^{13}C$ of soil CO_2, δ_ϕ is the $\delta^{13}C$ of soil-respired CO_2, and δ_a is the $\delta^{13}C$ of atmospheric CO_2. All δ values are relative to Vienna Pee Dee belemnite (VPDB). The temperature of calcite precipitation is set at 25°C, relating the carbon isotopic ratio of soil carbonate (δ_{cc}) to δ_s (*29*). As an independent objective metric of soil applicability, multiple (three or more) down-profile δ_{cc} measurements were made on each paleosol to reproduce the

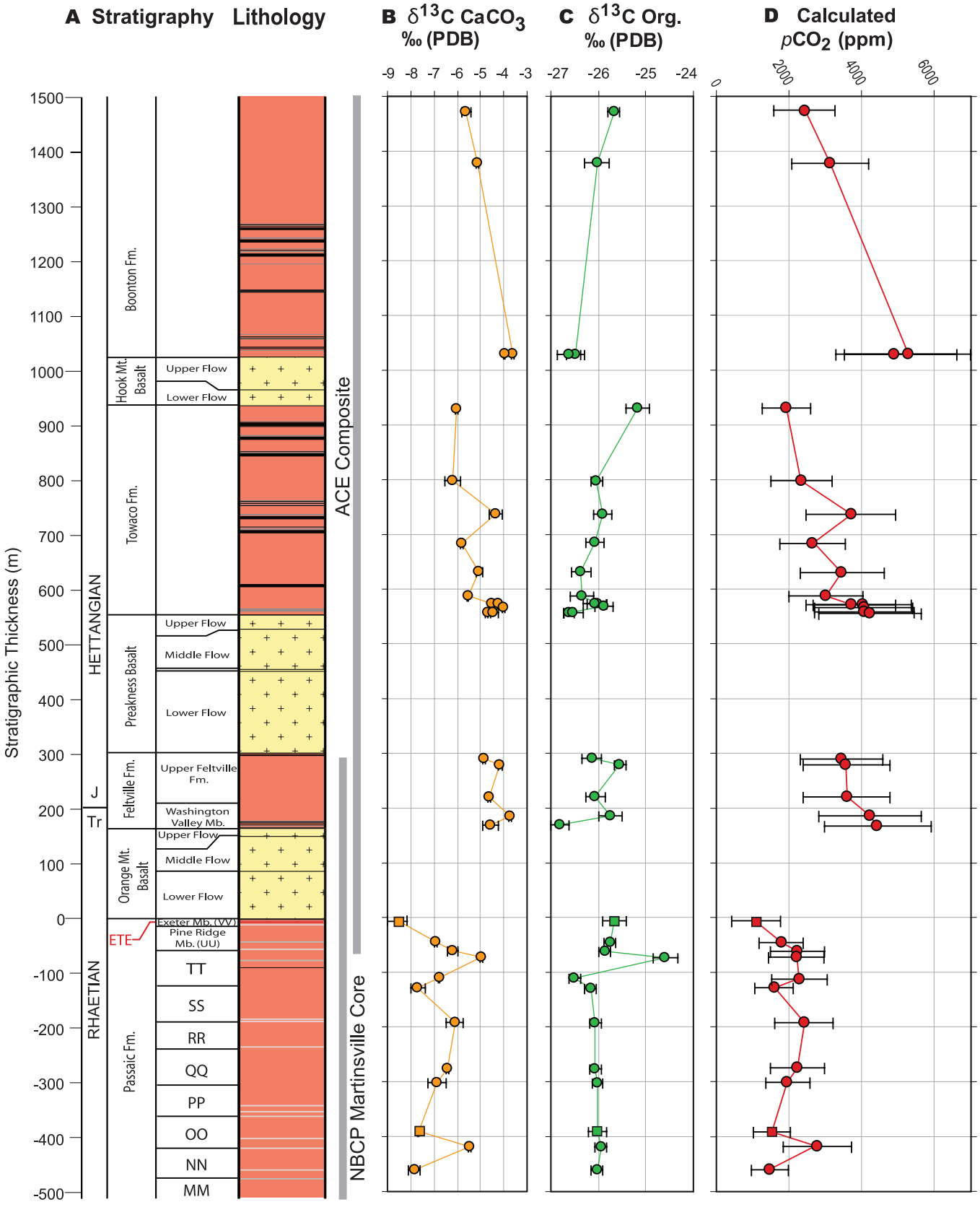

expected exponential decrease toward stabilization with depth (Fig. 2) (*29*, *31*). Using the mean of these soil-equilibrated measurements ensures that the mixing between the atmospheric and soil-respired reservoirs is at equilibrium with respect to the diffusion model. The measured carbon isotopic ratio of soil organic matter ($\delta^{13}C_{org}$) is related directly to δ_ϕ (*29*). Carbon-cycle perturbations are built into the model because the carbon isotopic ratio of the atmosphere (δ_a) is calculated from the measured $\delta^{13}C_{org}$ by assuming consistent fractionation by photosynthesis: $\delta_a = (\delta^{13}C_{org} + 18.67)/1.10$ (*32*). We use an $S(z)$ value of 3000 ± 1000 parts per million (ppm), appropriate for soils developed in a semi-arid climate with moderate productivity (*30*, *33*).

Atmospheric P_{CO_2} estimates in superposition with CAMP basalts. Pedogenic carbonates from the upper Passaic Formation deposited before the first CAMP volcanic unit (Orange Mountain Basalt) have $\delta^{13}C$ values generally below –5 per mil (‰) VPDB, with ±1.5‰ variability (Fig. 1B). The carbon isotopic composition of soil organic matter ($\delta^{13}C_{org}$) is remarkably stable around –26‰ (Fig. 1C), consistent with but less variable overall than results from independent analyses of wood and total organic carbon from elsewhere in the Newark and Hartford stratigraphy (*34*). Model results of the pedogenic carbonate paleobarometer yield P_{CO_2} estimates with a mean of ~2000 ppm [$S(z)$ = 3000 ppm] in the pre-CAMP stratigraphy (Fig. 1D). These estimates from over 500 m of the uppermost Passaic Formation, deposited over ~2.5 My of the latest Triassic (*18*, *19*), show internal consistency between outcrop and between cores and, with the tight stratigraphic resolution, suggest that there are no major CO_2-producing magmatic events before the observed Orange Mountain Basalt. This stable P_{CO_2} background is probably a measure of equilibrium continental silicate weathering in the Late Triassic.

The ~2000-ppm pre-CAMP P_{CO_2} baseline found in this study is not inconsistent with widely (geographically and stratigraphically) dispersed pedogenic carbonate estimates from elsewhere in the Newark Supergroup (*26*, *35*) or reconstructions from the Late Triassic Petrified Forest section (Fig. 3) (*8*). However, the Petrified Forest section lacks CAMP volcanics and can be correlated to the Newark succession only at the stage level (*36*), in which case the Rhaetian samples most likely overlap with the 2.5-My (*18*) pre-CAMP samples of this study but show considerably greater variability (500 to 3500 ppm) (Fig. 3). The high variability in the Petrified Forest section is probably due to the lack of down-profile isotope measurements and the use of temperatures estimated from the $\delta^{18}O$ of pedogenic calcite, which lacks a reliable calibration for use in the paleo record (*37*).

The carbon isotope value of pedogenic carbonate formed directly on top of the Orange Mountain Basalt (first flow unit) is enriched in ^{13}C by 1 to 2‰ above the pre-CAMP background (Fig. 1B). This increase and similar increases above the Preakness and Hook Mountain Basalts (the second and third flow units, respectively) reflect the increased influence of the atmospheric reservoir on soil carbonate formed at depth. Stratigraphically, above each flow unit, the carbon isotope composition of soil organic matter decreases by ~0.5 to 1.0‰, followed by a general return of $\delta^{13}C_{org}$ values to around –26‰, but with increased variability (Fig. 1C). The $\delta^{13}C$ values of pedogenic carbonate and soil organic matter directly above the Preakness Basalt have particularly good reproducibility between several laterally equivalent individual cored sections, allowing confidence in these measurements. Those soils formed on top of the Orange Mountain Basalt (Fig. 2B) show an increase in P_{CO_2} to 4400 ppm (Fig. 1D), which amounts to a doubling of P_{CO_2} above the pre-CAMP baseline. In every case, pedogenic carbonate samples of soils formed on the tops of the basaltic units yield P_{CO_2} estimates that are distinctly higher than the immediately pre-eruptive background levels (Fig. 1): 4200 ppm on top of the Preakness Basalt compared with 3000 ppm in the uppermost portion of the underlying Feltville Formation, and 5000 ppm directly on the Hook Mountain Basalt compared with 2500 ppm in the uppermost portion of the underlying Towaco Formation. This pattern suggests that the volcanism associated with each lava-flow unit had a direct effect on atmospheric P_{CO_2} by ~2000 ppm and was virtually immediate [to within the resolution of orbital precession (~20 ky)].

Chronostratigraphic control of P_{CO_2} estimates. A previous low-resolution reconstruction from the Newark Supergroup (two localities over 10 My) seemed to suggest relatively stable P_{CO_2} levels across the CAMP interval (*26*) and, when compared to our study, underscores the difficulty in attempting to capture a transient perturbation of the carbon system without adequate chronostratigraphic control (Fig. 3) (*38*, *39*). The stratigraphic level of the McCoy Brook sample of Tanner *et al*. (*26*) from the Fundy Basin is not known precisely (*40*), and it is quite possible that the soil formed long enough after emplacement of the North Mountain Basalt (correlative to the Orange Mountain Basalt) (*41*) that the full P_{CO_2} increase was not recorded. As demonstrated by this study, capturing such a transient signal

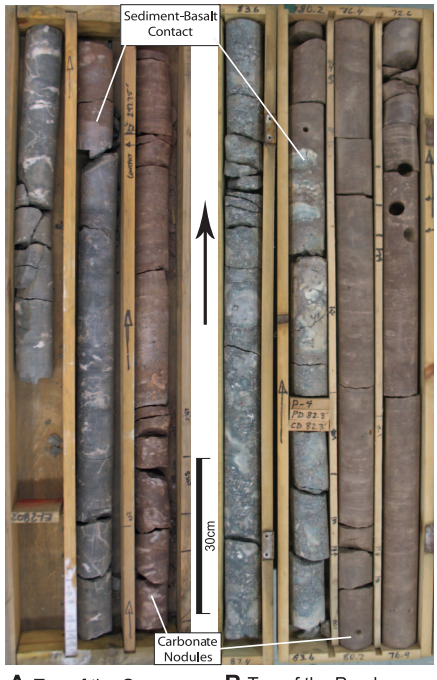

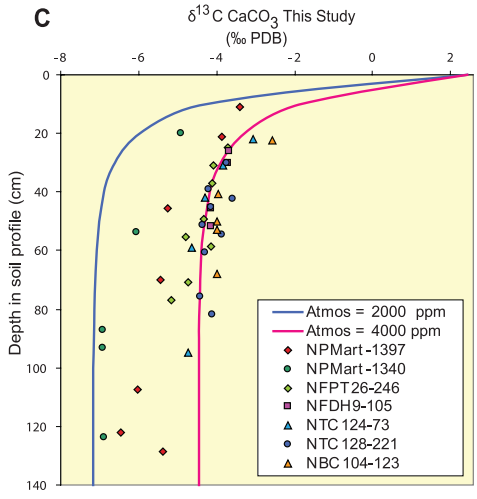

Fig. 2. Carbonate-bearing calcic vertisols formed directly on the tops of the lava flows; (**A**) on top of the Orange Mountain Basalt in ACE core PT-26, box 18; and (**B**) on top of the Preakness Basalt in ACE core C-124, box 3 (see Fig. 1 for stratigraphic column, fig. S1 for core locations). Scale bar, 30 cm. Depth in core decreases from left (deepest) to right (shallowest); up-core direction is indicated by the arrow; holes are soil-carbonate sampling locations. Such superposition removes any stratigraphic uncertainty from these P_{CO_2} estimates with regard to the flow units themselves. (**C**) Down-soil $\delta^{13}C$ profiles of pedogenic carbonates (δ_{cc}) from representative paleosols in the Passaic, Feltville, Towaco, and Boonton Formations used in this study (symbols encompass analytical error), compared with the δ_{cc} predicted by the diffusion model at atmospheric CO_2 concentrations of 2000 and 4000 ppm (blue and pink lines, respectively) [after (*31*)]. For this exercise only, atmospheric $\delta^{13}CO_2$ was set to −6.5‰, and soil $\delta^{13}C_{org}$ was set to −26.5‰, with an exponential production function and characteristic depth of production at 15 cm [see (*29*) for description of other parameters]. For all P_{CO_2} estimates made in this study, the $\delta^{13}C_{org}$ was measured directly and used as a model input. Soil carbonate above 20 cm in the profile was rare. Note that stabilization of measured δ_{cc} is often well below 50-cm soil depth. Using the mean of these depth-stabilized measurements ensures the mixing between the atmospheric and soil-respired reservoirs at equilibrium with respect to the diffusion model. Photographs of the soils used in (C), from samples NFPT26 and NTC124, are shown in (A) and (B).

requires <100-ky sampling resolution with respect to the volcanics. Other attempts to estimate P_{CO_2} over this interval, most notably the approximations using stomatal densities of leaf fossils from end-Triassic event boundary sections in Greenland and Sweden (*9*), indicate a doubling to tripling of P_{CO_2} from 800 to 2100 ppm (Fig. 3). These stomata-based estimates are substantially lower than those found here, but the stomata proxy is thought to underestimate P_{CO_2} (*42*), in which case a reported doubling to tripling broadly agrees with our findings and is corroborated by other cuticular estimates (*43*).

If the increase in P_{CO_2} after each major basaltic unit (Orange Mountain, Preakness, and Hook Mountain Basalts) can be ascribed to episodes of magmatic activity, which are likely to be very short (*22*), then the relatively high-resolution record of P_{CO_2} taken as a whole seems to require just the three distinct episodes of volcanism. This does not necessarily imply that the local thicknesses of the CAMP volcanics in the Newark are representative of the global volume of basalt produced by each flow unit. For example, although the Newark and Hartford Basins show three distinct volcanic episodes in nearly identical chronostratigraphic sequence (*41*, *44*), the thicknesses of the correlative flow units vary by a factor of 2. Nonetheless, the observed magnitude and singularity of the P_{CO_2} response to each flow unit in the Newark Basin implies that the magmatic events that produced them were regionally extensive and voluminous, because atmospheric CO_2 is globally homogeneous on the circulation time of the atmosphere. Although the second episode of magmatism produced the thickest lava flow unit (Preakness Basalt) in the Newark Basin, there is only a relatively small corollary increase in P_{CO_2}. Interestingly, a middle flow unit equivalent to the Preakness Basalt is not present in the South Atlas region of Morocco, whereas the uppermost flow unit there (Recurrent Basalt) is stratigraphically and geochemically equivalent to the Hook Mountain Basalt in the Newark Basin (*41*). Although the Hook Mountain Basalt is locally thin in the Newark, the associated P_{CO_2} increase is one of the largest recorded, implying that greater unrecorded volumes were erupted elsewhere. This body of evidence demonstrates the global applicability of the P_{CO_2} findings reported here; together, they make a compelling case that what has been recorded in the Newark Basin is a reasonable representation of a global sequence of events.

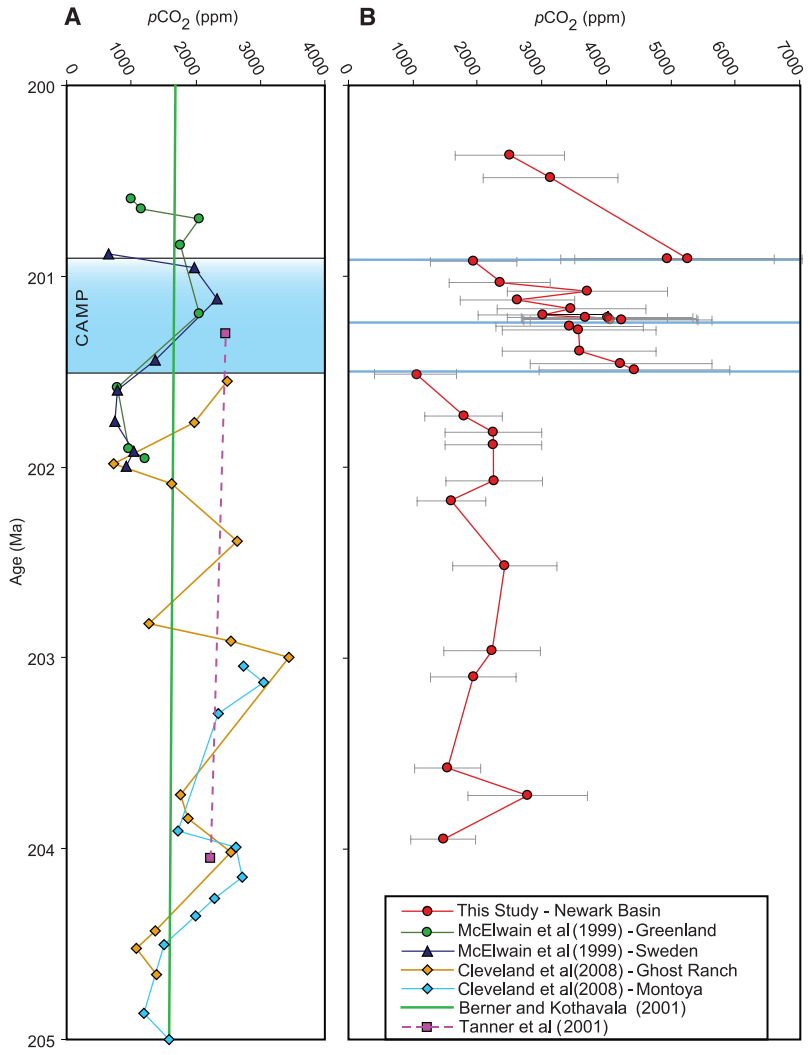

Fig. 3. (**A**) Atmospheric P_{CO_2} estimates previously made on Late Triassic and Early Jurassic sections using low-resolution pedogenic carbonates from other basins in the Newark Group (*26*) and the Rhaetian data of Cleveland *et al*. from the Petrified Forest section (*8*), stomatal densities from sections in Greenland and Sweden (*9*), and geochemical modeling (*50*). Approximate placement of the CAMP is shown in blue. The McElwain data were placed using the magnetic stratigraphy of Kent and Clemmensen (*51*) and Whiteside *et al*. (*34*). (**B**) P_{CO_2} estimates of this study with time [error bars are $S(z) = 3000 \pm 1000$ ppm]. The samples taken in this study are from the same series of ACE cores used to construct a time sequence through the magmatic interval in the Newark Basin (*22*). The heavy blue lines indicate the temporal placement (and duration) of each CAMP flow unit. Ma, million years ago.

To gauge the plausibility of a volcanic CO_2 source, we can compare the CO_2 efflux potential of the CAMP basalt volume to the effect observed in the Newark. Assuming a total CAMP volume of 2.4×10^6 km^3 (*27*) and a volcanic efflux of 1.4×10^{10} kg of CO_2 per km^3 (*7*), we estimate a total CO_2 degassing potential of 3.36×10^{16} kg CO_2. We focus on the lower volcanic unit (represented by the Orange Mountain Basalt in the Newark Basin), for which the pre-eruption background P_{CO_2} is well established. That initial pulse of activity represents roughly one-third of the total CAMP volume and, therefore, could have produced 1.12×10^{16} kg of CO_2, amounting to a ~1400-ppm increase in P_{CO_2} (at 7.82×10^{12} kg CO_2 per ppm). This instantaneous approximation is of the same order and within the error of our observed ~2000-ppm P_{CO_2} increase after the first major episode of CAMP volcanism, implying that the volcanic release of CO_2 was extremely rapid, which is consistent with the sporadic presence of only very thin and discontinuous sedimentary strata between flows (*21*, *41*). However, this does not preclude that a major component of the observed P_{CO_2} increase is contact metamorphic in origin (*45*), which is hinted at by the small decrease in $\delta^{13}C_{OM}$ above each flow unit.

The influence of basalt weathering. An intriguing phenomenon recorded by the Newark Basin paleosol sequence is the gradual apparent decrease in P_{CO_2} over time scales of 10^5 years after each successive episode of volcanism (Fig. 4). For example, elevated P_{CO_2} values just after the Preakness Basalt in the ~300-ky-long Towaco Formation have nearly returned to pre-eruptive levels by the emplacement of the succeeding Hook Mountain Basalt. We attribute the systematic decrease in P_{CO_2} as the enhanced response of continental silicate weathering consuming each volcanic input of CO_2 (*46*). Given the vast aerial extent of CAMP extrusive activity (*27*), it is plausible to attribute the rapidity of the decrease in atmospheric CO_2 to consumption by hydrolysis

of the CAMP volcanics themselves, especially in the tropical humid belt where the engines of continental weathering are most effective (*47*). Geochemical modeling of the period after emplacement of the Deccan LIP and its corresponding CO_2 input show a similar exponential decrease in P_{CO_2} due to consumption by weathering (Fig. 4) (*17*). Marine osmium isotope evidence also indicates that an increase in continental weathering followed the CAMP interval (*48*), lending credibility to a weathering hypothesis. Though the CAMP data correspond well to the initial stages of this modeled decrease, the uppermost portion of the Newark Basin section is truncated, so the full extent of this relation cannot be evaluated here.

Implications for the end-Triassic extinction. Neither the Feltville nor Towaco Formations show evidence of P_{CO_2} changes that can be associated with magmatic events other than those directly related to the observed volcanics. Similarly, the stability of P_{CO_2} estimates in the Pre-CAMP Passaic Formation leaves the ETE without an obvious P_{CO_2} precursor. However, the youngest sample in the pre-extrusive section (Exeter Member, Fig. 1) formed in a soil predating the first flow unit by only ~20 ky. This soil occurs two meters below the clay layer containing palynofloral evidence for the ETE in the same exposure, which itself predates the observed onset of volcanism in the Newark by ~19 ky (*24*). At these sedimentation rates, the uppermost paleosol sample that we studied in the Newark probably pre-dates the ETE by perhaps as little as ~1 ky. Therefore, it is possible that a pulse of CAMP volcanism and an attendant rapid rise in atmospheric P_{CO_2} with associated climatic implications occurred within the ~20-ky paleosol sampling gap before the age-equivalent of the Orange Mountain Basalt but remain undocumented. Nonetheless, the tight stratigraphic constraint implies that whatever phenomenon caused the ETE must have been very abrupt (occurring within a narrow thousand-year window) or have had minimal effect on atmospheric P_{CO_2} if it occurred earlier.

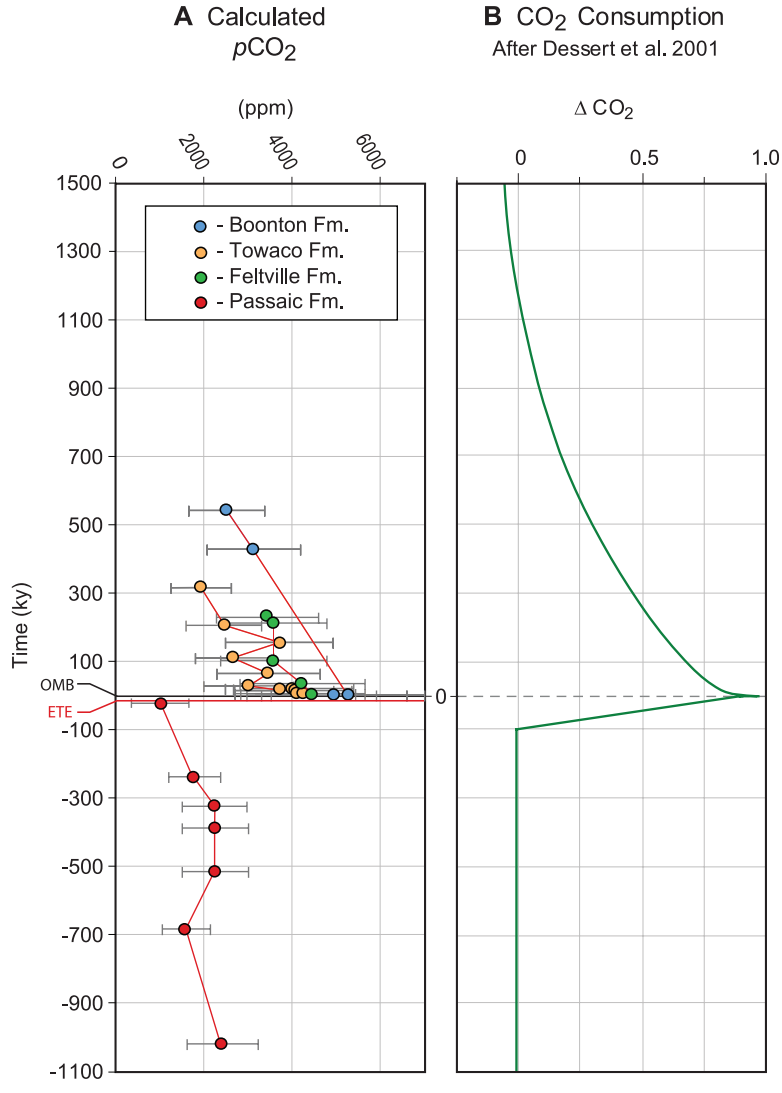

Fig. 4. (**A**) Calculated P_{CO_2} of this study versus time relative to the top of the Orange Mountain Basalt in the Newark Basin (the first CAMP flow unit). The P_{CO_2} estimates after each successive flow unit in the Newark have been normalized to the initial extrusive event for comparison to a silicate weathering model [colored symbols; error bars are $S(z)$ = 3000 ± 1000 ppm]. (**B**) Modeled CO_2 consumption due to weathering (*17*) after emplacement of the Deccan Traps. In the model, a pulse of CO_2 was added to the atmosphere (over 100 ky) accompanying the extrusion of the Deccan LIP. The change in P_{CO_2} represents the remaining fraction of the total P_{CO_2} increase in this particular modeling scenario. The abrupt increase of P_{CO_2} and subsequent postextrusive drawdown found in response to the CAMP volcanism in this study (A) is remarkably similar to the modeling results of Dessert *et al.* (*17*), bearing in mind the much longer interval of igneous activity assumed in the model.

References and Notes

1. M. F. Coffin, O. Eldholm, *Geology* **21**, 515 (1993).
2. J. B. Pollack *et al.*, *J. Geophys. Res.* **81**, 1071 (1976).
3. M. R. Rampino, R. B. Stothers, S. Self, *Nature* **313**, 272 (1985).
4. J. Hansen *et al.*, *Open Atmos. Sci. J.* **2**, 217 (2008).
5. D. L. Royer, R. A. Berner, I. P. Montanez, N. J. Tabor, D. J. Beerling, *Geol. Soc. Am. Today* **14**, 4 (2004).
6. K. Caldeira, M. R. Rampino, *Geophys. Res. Lett.* **17**, 1299 (1990).
7. S. Self, M. Widdowson, T. Thordarson, A. E. Jay, *Earth Planet. Sci. Lett.* **248**, 518 (2006).
8. D. M. Cleveland, L. C. Nordt, S. I. Dworkin, S. C. Atchley, *Geol. Soc. Am. Bull.* **120**, 1408 (2008).
9. J. C. McElwain, D. J. Beerling, F. I. Woodward, *Science* **285**, 1386 (1999).
10. P. B. Wignall, *Earth Sci. Rev.* **53**, 1 (2001).
11. V. Courtillot, C. Jaupart, I. Manighetti, P. Tapponnier, J. Besse, *Earth Planet. Sci. Lett.* **166**, 177 (1999).
12. V. E. Courtillot, P. R. Renne, *C. R. Geosci.* **335**, 113 (2003).
13. D. J. Beerling, B. H. Lomax, D. L. Royer, G. R. Upchurch Jr., L. R. Kump, *Proc. Natl. Acad. Sci. U.S.A.* **99**, 7836 (2002).
14. L. Nordt, S. Atchley, S. I. Dworkin, *Geology* **30**, 703 (2002).
15. A. Grard, L. M. Francois, C. Dessert, B. Dupre, Y. Godderis, *Earth Planet. Sci. Lett.* **234**, 207 (2005).
16. H. Svensen *et al.*, *Earth Planet. Sci. Lett.* **277**, 490 (2009).
17. C. Dessert *et al.*, *Earth Planet. Sci. Lett.* **188**, 459 (2001).
18. D. V. Kent, P. E. Olsen, *J. Geophys. Res. Solid Earth* **104**, 12831 (1999).
19. P. E. Olsen, D. V. Kent, B. Cornet, W. K. Witte, R. W. Schlische, *Geol. Soc. Am. Bull.* **108**, 40 (1996).
20. A. Marzoli *et al.*, *Science* **284**, 616 (1999).
21. P. E. Olsen, D. V. Kent, M. Et-Touhami, J. Puffer, in *The Central Atlantic Magmatic Province: Insights from Fragments of Pangea*, W. Hames *et al.*, Eds. (American Geophysical Union, Washington, DC, 2003), Geophysical Monograph vol. 136, pp. 7–32.
22. P. E. Olsen, R. W. Schlische, M. S. Fedosh, in *The Continental Jurassic*, M. Morales, Ed. (Museum of Northern Arizona, Flagstaff, AZ, 1996), bulletin no. 60, pp. 11–22.
23. S. J. Fowell, B. Cornet, P. E. Olsen, in *Pangaea: Paleoclimate, Tectonics and Sedimentation During Accretion, Zenith and Break-Up of a Supercontinent*, G. D. Klein, Ed. (Geological Society of America, Boulder, CO, 1994), Geological Society of America Special Paper, vol. 288, pp. 197–206.
24. P. E. Olsen *et al.*, *Science* **296**, 1305 (2002).
25. T. E. Cerling, *Global Biogeochem. Cycles* **6**, 307 (1992).
26. L. H. Tanner, J. F. Hubert, B. P. Coffey, D. P. McInerney, *Nature* **411**, 675 (2001).
27. J. G. McHone, in *The Central Atlantic Magmatic Province: Insights from Fragments of Pangea*, W. Hames *et al.*, Eds.

(American Geophysical Union, Washington, DC, 2003), Geophysical Monograph vol. 136, pp. 241–254.
28. W. S. Holbrook, P. B. Kelemen, *Nature* **364**, 433 (1993).
29. Detailed methodology and all original analytical data are available as supporting material on *Science* Online.
30. T. E. Cerling, in *Palaeoweathering, Palaeosurfaces and Related Continental Deposits*, M. Thiry, R. Simon-Coinçon, Eds. (Special Publications of the International Association of Sedimentologists, Oxford, 1999), vol. 27, pp. 43–60.
31. J. Quade, T. E. Cerling, J. R. Bowman, *Geol. Soc. Am. Bull.* **101**, 464 (1989).
32. N. C. Arens, A. H. Jahren, R. Amundson, *Paleobiology* **26**, 137 (2000).
33. D. O. Breecker, Z. D. Sharp, L. D. McFadden, *Geol. Soc. Am. Bull.* **121**, 630 (2009).
34. J. H. Whiteside, P. E. Olsen, T. Eglinton, M. E. Brookfield, R. N. Sambrotto, *Proc. Natl. Acad. Sci. U.S.A.* **107**, 6721 (2010).
35. R. K. Suchecki, J. F. Hubert, C. C. B. De Wet, *J. Sediment. Petrol.* **58**, 801 (1988).
36. D. M. Cleveland, S. C. Atchley, L. C. Nordt, *J. Sediment. Res.* **77**, 909 (2007).
37. S. I. Dworkin, L. Nordt, S. Atchley, *Earth Planet. Sci. Lett.* **237**, 56 (2005).
38. D. Beerling, *Nature* **415**, 386 (2002).
39. G. J. Retallack, *Nature* **415**, 387 (2002).
40. L. H. Tanner, *The Great Rift Valleys of Pangea in Eastern North America*, P. M. L. Tourneau, P. E. Olsen, Eds. (Columbia Univ. Press, New York, 2003).
41. J. H. Whiteside, P. E. Olsen, D. V. Kent, S. J. Fowell, M. Et-Touhami, *Palaeogeogr. Palaeoclimatol. Palaeoecol.* **244**, 345 (2007).
42. D. J. Beerling, D. L. Royer, *Annu. Rev. Earth Planet. Sci.* **30**, 527 (2002).
43. G. J. Retallack, *Nature* **411**, 287 (2001).
44. P. E. Olsen, *U.S. Geol. Surv. Bull.* **1776**, 6 (1988).
45. H. Svensen *et al.*, *Nature* **429**, 542 (2004).
46. J. C. G. Walker, P. B. Hays, J. F. Kasting, *J. Geophys. Res.* **86**, 9776 (1981).
47. C. Dessert, B. Dupre, J. Gaillardet, L. M. Francois, C. J. Allegre, *Chem. Geol.* **202**, 257 (2003).
48. A. S. Cohen, A. L. Coe, *Palaeogeogr. Palaeoclimatol. Palaeoecol.* **244**, 374 (2007).
49. M. S. Fedosh, J. P. Smoot, *U.S. Geol. Surv. Bull.* **1776**, 19 (1988).
50. R. A. Berner, Z. Kothavala, *Am. J. Sci.* **301**, 182 (2001).
51. D. V. Kent, L. B. Clemmensen, *Bull. Geol. Soc. Den.* **42**, 121 (1996).
52. We are grateful to J. Quade and P. E. Olsen for their numerous helpful discussions and L. Godfrey for her technical lab assistance. This research was supported by 2009 Geological Society of America and the Society of Economic Mineralogists and Petrologists Graduate Research Awards and NSF grant EAR 0958867. This work is Lamont-Doherty Earth Observatory Contribution #7432.

Supporting Online Material

www.sciencemag.org/cgi/content/full/science.1199011/DC1
Materials and Methods
Fig. S1
Table S1
References

13 October 2010; accepted 2 February 2011
Published online 17 February 2011;
10.1126/science.1199011

CRYPTOCHROME Is a Blue-Light Sensor That Regulates Neuronal Firing Rate

Keri J. Fogle, Kelly G. Parson, Nicole A. Dahm, Todd C. Holmes*

Light-responsive neural activity in central brain neurons is generally conveyed through opsin-based signaling from external photoreceptors. Large lateral ventral arousal neurons (lLNvs) in *Drosophila melanogaster* increase action potential firing within seconds in response to light in the absence of all opsin-based photoreceptors. Light-evoked changes in membrane resting potential occur in about 100 milliseconds. The light response is selective for blue wavelengths corresponding to the spectral sensitivity of CRYPTOCHROME (CRY). *cry*-null lines are light-unresponsive, but restored CRY expression in the lLNv rescues responsiveness. Furthermore, expression of CRY in neurons that are normally unresponsive to light confers responsiveness. The CRY-mediated light response requires a flavin redox-based mechanism and depends on potassium channel conductance, but is independent of the classical circadian CRY-TIMELESS interaction.

The *Drosophila melanogaster* circadian clock circuit is composed of 140 to 150 neurons in the central brain and includes PIGMENT-DISPERSING FACTOR (PDF)–expressing lateral ventral neurons. The large lateral ventral neurons (lLNvs) are arousal neurons (*1*–*3*) and increase spontaneous action potential firing in response to light (*4*), whereas the small lateral ventral neurons (sLNvs) are critical for circadian function (*5*). Light resets the circadian clock via two mechanisms (*6*): rhodopsin-based external photoreceptors [the compound eye, ocelli, and the Hofbauer-Buchner (HB) eyelet] and the blue-light photopigment CRYPTOCHROME (CRY). *Drosophila* CRY is best known for its light-activated targeting of TIMELESS (TIM) for degradation, resetting the clock (*7*–*9*). External photoreceptors and CRY entrain the *Drosophila* circadian circuit at vanishingly low light levels (*10*, *11*). CRY also mediates magnetosensitivity in flies and butterflies (*11*–*13*).

In addition to the circadian molecular clock, membrane excitability is a key component of normal maintenance of circadian rhythms (*14*). Electrophysiological characterization of the s- and lLNvs has shown that their membrane properties are circadian-regulated outputs as well. Spontaneous firing frequencies are higher during the early day, gradually drop until dusk, and then rise again through the course of the night (*1*, *15*). Additionally, the lLNv spontaneous firing frequency elevates 20 to 200% in response to moderately bright light (*4*). Given the plurality of light inputs to the lLNv, we investigated the lLNv electrophysiological light response (*16*) and found that the response is due to CRY acting by a cell-autonomous, redox-based mechanism, independent of CRY-TIM interactions, which requires the conductance of membrane potassium channels. Furthermore, ectopic expression of CRY optogenetically confers electrophysiological light responsiveness to neurons that ordinarily do not respond to light.

Results. Both tonic and burst firing lLNvs recorded in the whole-cell current clamp configuration in an acutely dissected whole-brain preparation from flies expressing the *pdfGAL4* driver and green fluorescent protein (GFP)–tagged nonconducting UAS-dORK, a *Drosophila* membrane-delimited potassium channel (*4*, *14*), (*pdfGAL4-NC1-GFP*) under dark conditions (>0.02 mW/cm^2) immediately increased their firing rate and their resting membrane potential in response to moderate-intensity white light (4 mW/cm^2) (Fig. 1A, top) or high-intensity blue light (19 mW/cm^2) from a mercury light source (450 to 490 nm) (Fig. 1A, bottom), then rapidly returned to baseline firing rate upon return to darkness. The strength of the firing frequency lLNv light response, expressed here as the firing frequency with the lights on divided by the firing frequency with the lights off (FF on/FF off), varied with light intensity, exhibiting significantly higher firing frequency during lights on compared with lights off at intensities of 2 to 3 mW/cm^2 or higher (Fig. 1B). FF on/off for 19 mW/cm^2 was 1.62 ± 0.14 (n = 11) for 4 to 5 mW/cm^2 was 1.51 ± 0.15 (n = 18), for 2 to 3 mW/cm^2 was 1.39 ± 0.06 (n = 68), for 1 to 2 mW/cm^2 was 1.18 ± 0.02 (n = 27), for 0.6 mW/cm^2 was 1.23 ± 0.06 (n = 16), and for 0.3 mW/cm^2 was 1.10 ± 0.04 (n = 13). Light responses to intensities of 19 mW/cm^2, 4 to 5 mW/cm^2, and 2 to 3 mW/cm^2 were significantly different from 1 to 2 mW/cm^2 [P = < 0.0001, 0.006, and 0.02, respectively, by analysis of variance (ANOVA)].

The lLNvs anatomically appear to receive input from the compound eyes and the HB eyelet. To determine whether the lLNv light response is due to synaptic inputs from external opsin-based photoreceptors, we recorded lLNv in *glass60j* (*gl60j*) mutant flies, which lack all external photoreceptors because of a null mutation in the *eyeless* gene (*6*). The lLNv response to moderate-intensity white light for *gl60j* flies was 1.37 ± 0.09 (n = 14; P = 0.81

Department of Physiology and Biophysics, University of California Irvine, Irvine, CA 92697, USA.

*To whom correspondence should be addressed. E-mail: tholmes@uci.edu